TECHNICAL REPORT

nature neuroscience

FACS-array profiling of striatal projection neuron subtypes in juvenile and adult mouse brains

Mary Kay Lobo[1,2], Stanislav L Karsten[1–3], Michelle Gray[1,2], Daniel H Geschwind[1–3] & X William Yang[1,2]

A major challenge in systems neuroscience is to perform precise molecular genetic analyses of a single neuronal population in the context of the complex mammalian brain. Existing technologies for profiling cell type–specific gene expression are largely limited to immature or morphologically identifiable neurons. In this study, we developed a simple method using fluorescent activated cell sorting (FACS) to purify genetically labeled neurons from juvenile and adult mouse brains for gene expression profiling. We identify and verify a new set of differentially expressed genes in the striatonigral and striatopallidal neurons, two functionally and clinically important projection neuron subtypes in the basal ganglia. We further demonstrate that Ebf1 is a lineage-specific transcription factor essential to the differentiation of striatonigral neurons. Our study provides a general approach for profiling cell type–specific gene expression in the mature mammalian brain and identifies a set of genes critical to the function and dysfunction of the striatal projection neuron circuit.

The extraordinary complexity and heterogeneity of the mammalian nervous system significantly limits the power of the microarray for gene expression analyses. Because many distinct neuronal and non-neuronal cells are highly intermixed, microarray analyses of a given brain region either during development, behavioral or pharmacological manipulation or subsequent to a disease process only provide a composite view of gene expression. For example, if a gene is expressed at low or moderate levels in a single cell type, even a large change in its expression may not be detected because it is below the abundance level measurable by microarrays. Additionally, changes in gene expression in one cell type may be masked by apposing changes in another cell type. Thus, critical and significant gene expression alterations within a single neuronal population often elude detection in microarray analyses using complex brain tissues[1–3]. Even when such expression changes are identified in experiments using whole brain tissue, we must rely on extensive *post-hoc* analysis to determine whether they are caused by changes in cellular composition, whether they reflect a change in gene expression within a subset of cells or all cells, or a combination of both.

Microarray studies using purified neuronal populations provide a powerful alternative to study cell type–specific gene expression in the mammalian brain. Existing methodologies for cell type–specific gene expression profiling, including the use of single neurons[4], laser-captured neurons[5] and neurons that are retrogradely labeled with fluorescent tracers and purified by FACS (ref. 6), can be effective in many cases and have led to significant biological insights[6–8]. Although these methodologies are suitable for use with certain applications, they are relatively labor intensive and have not yet been assessed in the mature brain, particularly in expression profiling of adjacent, morphologically indistinguishable neuronal subtypes within brain regions that are highly heterogenous[1–3]. Recent advances in bacterial artificial chromosome (BAC)-mediated transgenesis in mice[9–11] allow relatively high-throughput genetic labeling of distinct neuronal populations in the brain using fluorescent reporter proteins (gene expression nervous system atlas, GENSAT; ref. 12). It is therefore particularly important to develop a parallel and highly efficient methodology that could use this invaluable resource for cell type–specific expression profiling in the developing and mature mammalian brain.

In this study, we developed a simple method to purify juvenile and adult genetically labeled neurons from the GENSAT BAC transgenic mice for gene expression profiling. As a proof of principle, we chose to focus on the striatal projection neurons in the basal ganglia because of their critical roles in motor control and habit and reward learning[13–15], and because their dysfunction has been implicated in major neurological and psychiatric disorders[16–23]. In the striatum, a major nucleus of the basal ganglia, 95% of the neurons are projection neurons called medium spiny neurons (MSNs). These neurons are further subdivided into two morphologically indistinguishable and mosaically distributed neuronal subtypes: striatonigral MSNs (the direct pathway) and striatopallidal MSNs (the indirect pathway) (refs. 13,14,16). Current models of basal ganglia function suggest that these two projection neuron pathways provide balanced but antagonistic influences on the basal ganglia output and behavior: the direct pathway promotes movement and the indirect pathway inhibits movement[13,14,16]. The importance of these distinct pathways is further illustrated by a wide body of literature that implicates their functional imbalance in movement disorders including Parkinson disease, Huntington disease,

[1]Center for Neurobehavioral Genetics, Semel Institute for Neuroscience and Human Behavior; Department of Psychiatry and Biobehavioral Sciences, [2]Brain Research Institute and [3]Progam in Neurogenetics, Department of Neurology, David Geffen School of Medicine, University of California at Los Angeles (UCLA), 695 Charles Young Drive South, Gonda 3506B, Los Angeles, California 90095, USA. Correspondence should be addressed to X.W.Y. (xwyang@mednet.ucla.edu).

Received 11 October 2005; accepted 25 January 2006; Published online 19 February 2006; doi:10.1038/nn1654

Tourette syndrome and dystonia[16–18]. These projection neurons are also implicated in major psychiatric disorders including schizophrenia, depression, obsessive and compulsive disorders (OCD) and drug addiction[19–23].

Despite their functional and clinical importance, the molecular basis for the differential function of these striatal projection neuron pathways remains largely unknown, with only a few notable exceptions[24–27]: these include the enrichment of dopamine receptor D1 (Drd1a), muscarinic receptor M4 (Chrm4) and tachykinin 1 (Tac1; also known as substance P) in the striatonigral neurons, and the enrichment of preproenkephalin 1 (Penk1), dopamine receptor D2 (Drd2) and adenosine receptor A2a (Adora2a) in the striatopallidal neurons. In this study, we used FACS to efficiently purify mature genetically labeled striatial projection neuron subtypes from GENSAT BAC transgenic mice for microarray studies. Using this technology (which we called FACS-array), we demonstrate the ability to identify reproducible gene expression differences between these MSN subtypes, even in neurons sorted from the adult mice. We verified a new set of genes with restricted expression in MSN subtypes and demonstrated that the transcription factor Ebf1 is expressed in a striatonigral-specific fashion and is a critical determinant in striatonigral neuron differentiation.

RESULTS

FACS-array profiling of MSN subtypes

We first developed and applied an efficient method to purify genetically labeled MSN subtypes for microarray studies using GENSAT BAC transgenic mice. These mice contained cell type–specific regulatory elements that express enhanced green fluorescent protein (EGFP) specifically in MSN subtypes[12]: in *Drd2-EGFP* mice (*D2* mice), the striatopallidal neurons were labeled; and in *Drd1a-EGFP* and *Chrm4-EGFP* mice (*D1* and *M4* mice), the striatonigral neurons were labeled (**Fig. 1**). Because these MSNs reach adult-like distribution and undergo the final stages of circuitry development at postnatal day 20 (P20; ref. 28), we initially used P20 mice for the study, reasoning that it would be easier to sort juvenile neurons in these mice rather than adult neurons. In each experiment (**Fig. 2a**), striatal slices from 3–4 transgenic mice were enzymatically dissociated, labeled with propidium iodide (PI) to identify dead neurons and sorted to purify $EGFP^+$ and PI^- neurons, typically yielding 5,000–10,000 EGFP-labeled MSNs (**Fig. 2b,c**). RNA was prepared from the sorted neurons; typically, the yield was 3–10 ng RNA per sort. RNA quality was assessed using the Agilent Bioanalyzer Picochip (**Fig. 2d**). Semiquantitative reverse transcriptase polymerase chain reaction (RT-PCR; **Fig. 2e**) and quantitative RT-PCR (qRT-PCR, **Supplementary Table 1** online) showed that the expression of all six known MSN subtype–specific genes was consistently segregated in these RNA samples (*Drd1a* data not shown), demonstrating that each sorted RNA sample is truly cell type specific with little cross-contamination from the other intermixed MSN subtype.

The cell type–specific RNA was then used to profile differential gene expression in the two MSN subtypes. Five independent experiments were performed at P20 to compare three *D2*- to three *M4*-sorted samples and two *D2*- to two *D1*- sorted samples (**Fig. 3a**; **Supplementary Table 1**). In each independent experimental comparison, sorted cells from 3–4 transgenic mice of a given genotype were compared to cells from 3–4 transgenic mice of the other genotype (**Fig. 3a**). To demonstrate the reproducibility of the reported microarray experiments, we performed homotypic comparisons (that is, comparisons between independent biological replicates hybridized onto different arrays). This encompasses the full range of biological variability due to individual animals, the enzymatic dissociation, FACS sorting, RNA amplification and array hybridization (including array to array variability), providing us with an empiric false discovery rate[26]. The average correlation between independent biological replicates was 0.98 for homotypic comparisons ($n = 12$) and 0.97 for heterotypic comparisons ($n = 16$), with slopes ranging from 0.97 to 1.01 (**Fig. 3b**). This demonstrated robust reproducibility across independent experimental samples with the FACS-array procedure.

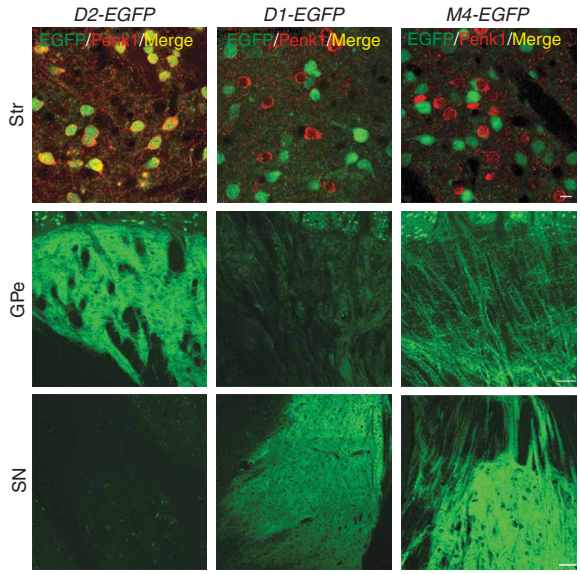

Figure 1 EGFP expression in subtypes of striatal projection neurons in three BAC transgenic mice. Top, double immunofluorescence of EGFP (green) and Penk1 (red; labeling striatopallidal neurons) in P20 striatum. Middle and bottom, EGFP fluorescence illustrating axonal projections and terminals in the BAC mice in either the globus pallidus externa (GPe) or the substantia nigra (SN). These results confirmed that in *D2-EGFP* mice, the striatopallidal neurons are specifically labeled, and in *D1-EGFP* and *M4-EGFP* mice, the striatonigral neurons are specifically labeled. Scale bars: top, 10 μm; middle and bottom, 100 μm.

For the identification of differential expression in heterotypic comparisons (different MSN subtypes), the genes were required to pass two relatively conservative criteria: a ratio beyond the 95% confidence interval observed in homotypic comparisons[29], which corresponded to a ratio of twofold differential expression, and a paired *t*-test corrected for multiple comparisons at a false discovery rate of 0.05 ($P < 0.01$). We identified eight genes enriched in striatonigral neurons and 23 genes enriched in striatopallidal neurons when we required that the criteria for differential expression be met in 4 of 5 comparisons (**Table 1**). We identified an additional ten differentially expressed genes when we required that the criteria be met in only 3 of 5 comparisons (**Table 1**). These genes are also highly likely to be differentially expressed, because 3 of 3 genes tested from this additional list were confirmed by RT-PCR (see below and **Table 1**). Additionally, out of the six genes previously known to be differentially expressed, *Penk1* and *Adora2a* were identified based on the stringent criteria, providing a valuable initial validation. Although only two of the six known genes were identified in the P20 experiment, all the other known genes were differentially enriched in the sorted RNA samples by RT-PCR (**Fig. 2e** and **Supplementary Table 2** online), suggesting that low gene expression levels, poor array probe design or both may contribute to the false negatives in the experiment.

To evaluate whether the dissociation and FACS procedure can introduce reactive changes including apoptosis, which may

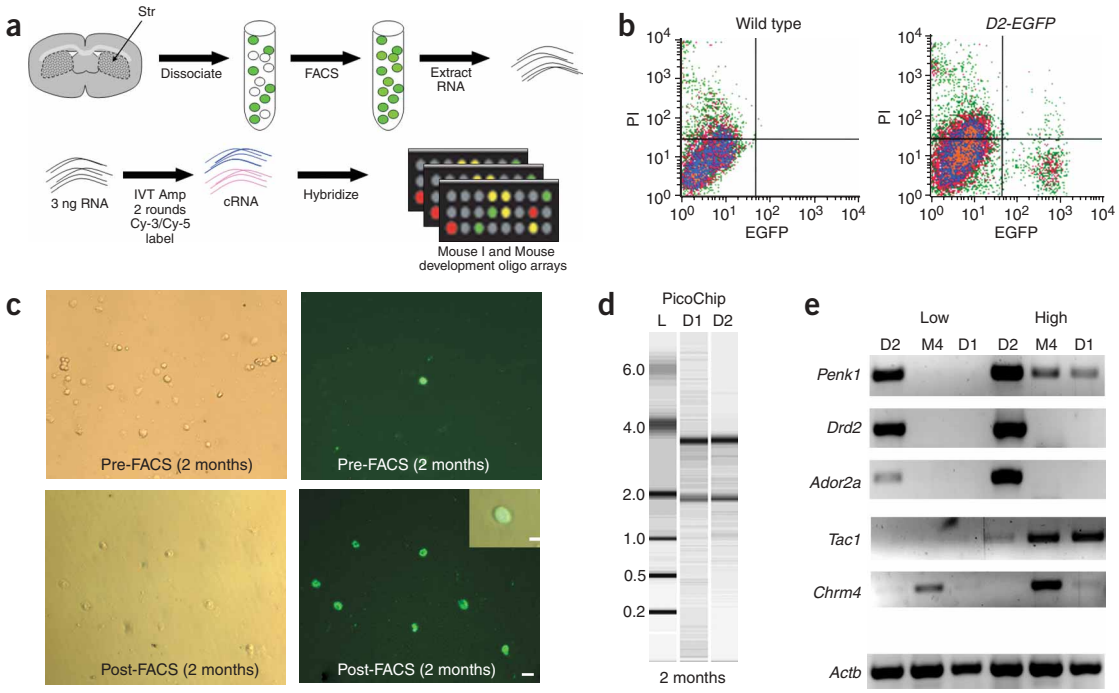

Figure 2 FACS-array procedure and validation of known striatal genes. (**a**) Schematic drawing of the FACS-array procedure to dissect live striata from transgenic mice, enzymatically dissociate the striatal neurons and use FACS to purify EGFP$^+$ and PI$^-$ MSNs for preparation of RNA and cRNA. The cRNA from two different MSN subtypes (blue and pink) was labeled with Cy-3 and Cy-5 fluorescent dye and hybridized to the microarrays. (**b**) An example of FACS purification of EGFP$^+$ and PI$^-$ MSNs. Left and right, sorting of MSNs from the wild-type and transgenic mice, respectively. EGFP$^+$ and PI$^-$ MSNs are located in the lower right quadrant in the sorting from transgenic mice. (**c**) Imaging of neurons from 2-month-old *D2-EGFP* mice before and after FACS. FACS-sorted cells remained morphologically similar to presorted cells and were 100% EGFP$^+$. Scale bar, 20 μm except for inset (10 μm). (**d**) Analysis of RNA isolated from MSNs of 2-month-old *D2* and *D1* mice. RNA ladder spans 0.2–6.0 kb. (**e**) Semiquantitative RT-PCR using RNA samples prepared from *D2*-, *M4*- or *D1*-sorted MSNs demonstrated proper amplification of five known marker genes that are differentially expressed in the MSN subtypes. β-actin was used as a loading control. PCR products were amplified using two different cycles: low cycles (low) were 37 cycles for *Drd2*, *Adora2a* and *Chrm4*, and 27 for *Penk1*, *Tac1* and *Actb*; high cycles (high) were 42 cycles for *Drd2*, *Adora2a* and *Chrm4*, and 32 for *Penk1*, *Tac1* and *Actb*.

confound the FACS-array results, we performed over-representation analyses for cell-death–related genes expressed in the sorted cells (D1, D2 and M4) versus whole brain tissues such as brain stem, cortex, spinal cord and cerebellum (**Supplementary Fig. 1** online). None of the gene categories related to cell death or apoptosis were enriched in the P20 sorted cells, nor was there a trend for statistical significance in any category (data not shown), suggesting that the FACS-array procedure *per se* does not arbitrarily introduce significant reactive gene expression changes.

Gene Ontology (GO) analyses[30] demonstrated that intracellular signaling pathways are significantly enriched in this list of genes ($P < 0.05$; **Supplementary Fig. 2** online), a surprising result given the small number of differentially expressed genes used for this analysis. Thus, GO analyses suggested that differential signaling is critical to the function of these two MSN subtypes, as has been previously proposed[13,31]. Notably, most of the MSN subtype–specific genes have molecular functions that are not represented by the few genes already known to distinguish between these two MSN subtypes; these include genes encoding transcription factors (*Zfp521*, *Nr4a1* and *Arx*), signal transduction molecules (*Gnb4*, *Gnb5*, *Dock3*, *Map3K4* and *Rgs2*), cell-cell signaling molecules (*Nrxn1*, *Plxdc1* and *Lrrn6c*), RNA binding proteins (*Qk* and *Arpp19*), metabolic enzymes (*Upb1*, *Adk* and *Ctsz*) and a nucleotide sugar transporter (*Slc35d3*). Moreover, *in situ* hybridization analyses from existing databases (GENSAT; Allen Brain Atlas) as well as by us (**Table 1** and **Supplementary Fig. 3** online) showed that the expression of nine of the newly identified genes was relatively enriched in the striatum. These genes thus constituted a short list of candidate genes critical to maturation and function of the distinct striatal projection neuron subtypes.

Our FACS-array analyses of P20 MSN subtypes demonstrated that we can reproducibly identify a set of differentially expressed genes in these juvenile neurons, which are still undergoing the final stages of neuronal differentiation. We next investigated whether FACS could be extended to purify adult neurons for microarray studies, which would provide an even more useful technical advance, particularly for behavioral studies and disease research[1]. It is feasible to FACS-purify developing and immature neurons as well as neuronal precursors for microarray analyses[6], but this technique has not been assessed in fully mature adult neurons (45 d or older in mice). We performed two independent microarray experiments (two *D2*- versus two *D1*-sorted samples) using 2-month-old mice to see whether we could identify a significant subset of the differences detected in the striatal projection neurons sorted at P20, as a proof of principle. Notably, 19 new genes on the initial list from P20 mice also showed greater than twofold enrichment in appropriate cell types in the adult mice. There was a highly significant overlap of genes detected at both ages in specific MSN subtypes ($P < 0.001$, χ^2-test; **Table 1**). Three of the genes already known to distinguish these two MSN subtypes, *Penk1*, *Adora2a* and *Tac1* (substance P), were enriched 57.5-fold, 2.8-fold and 4.8-fold in appropriate cell types in the adult mice. These results validated a substantial number of genes as being MSN subtype–enriched genes in the adult. Furthermore, they demonstrated for the first time that one

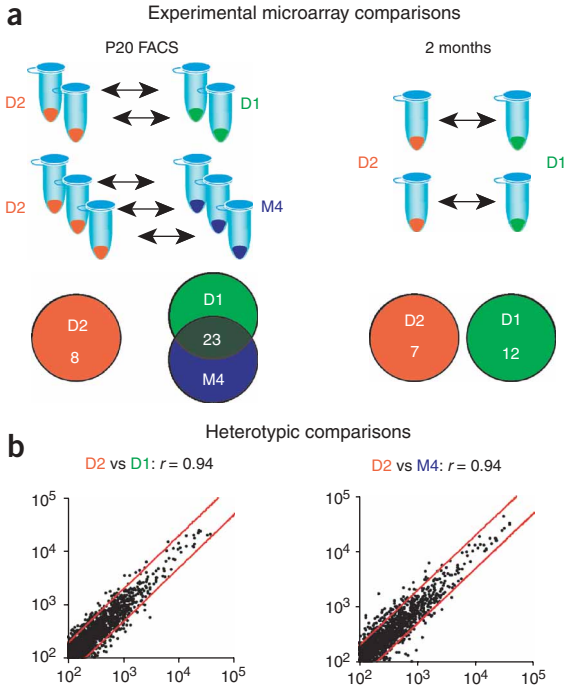

Figure 3 Microarray comparison schematic. (**a**) Experimental design for P20 and 2- month comparisons. Each tube represents pooled RNA from *D1*-, *D2*- or *M4*-sorted MSNs from 3 or 4 mice of a given genotype that were being compared in the microarray experiment. Thus, a total of 5 independent experiments (2 *D2* versus *D1*; 3 *D2* versus *M4*) were performed with dye swapping at P20; 2 (*D2* versus *D1*) were done at 2 months of age; 12 microarrays in total. (**b**) Correlation plots of two representative heterotypic comparisons from *M4* versus *D2* sorts, and *D1* versus *D2* sorts. Red lines, differential expression threshold. Values on the *x*- and *y*-axes represent normalized signal intensities.

could reliably and efficiently profile neuronal cell type–specific gene expression in the adult mouse brain and extract biologically meaningful data using FACS-sorted genetically labeled neurons.

Independent validation of the FACS-array results

We next used independent methods to validate a subset of MSN subtype–specific genes, focusing on genes that were differentially regulated in both P20 and adult arrays and/or striatal specific. First, we used semiquantitative RT-PCR and validated the direction of cell type enrichment in 18 of 23 differentially regulated genes on our list (**Table 1**; **Fig. 4a** and **Supplementary Table 2**). As expected, most of these genes were expressed in both MSN subtypes but were enriched in a specific MSN subtype. In addition, four of the genes in this assay were consistently restricted to a single MSN subtype. These were *Slc35d3* and *Qk*, which are specific to the striatonigral neurons, and *Dock3* and *Hbegf*, which are specific to the striatopallidal neurons.

To directly visualize the differential cellular distribution of a few of the newly identified genes in the striatum, we performed double *in situ* hybridizations in a subset of these genes: nonradioactive *in situ* hybridization with a *Penk1* probe to label the striatopallidal neurons and radioactive *in situ* hybridization to detect the candidate genes. The control *in situ* hybridization of *Penk1/Penk1* and *Tac1/Penk1* showed appropriate clustering of the grains relative to the *Penk1*$^+$ cells (**Fig. 4b**). Double *in situ* hybridization confirmed *Dock3* specificity for the striatopallidal neurons; *Slc35d3*, *Gnb4* and *Stmn2* had radioactive grains clustered outside the *Penk1*$^+$ cells, consistent with their restriction to the striatonigral neurons. In summary, a substantial number of genes identified in the microarray studies were independently verified using semiquantitative RT-PCR and a few were further characterized by double *in situ* hybridization.

Genetic validation of *Slc35d3* expression *in vivo*

A major motivation for this study was to identify molecular candidates critical to the postnatal maturation and function of these two important striatal projection neuron subtypes. For this purpose, we initially pursued more detailed genetic analyses of two genes as a proof of principle. One of the most interesting genes revealed in this study was *Slc35d3*, a gene encoding an uncharacterized nucleotide sugar transporter. Members of the *Slc35* family transport specific subsets of nucleotide sugars into the endoplasmic reticulum and Golgi for protein glycosylation[32]. Two *Slc35* homologs in *Drosophila melanogaster*[33,34] and *Caenorhabditis elegans*[35] are rate-limiting regulators of protein glycosylation, controlling the function of key developmental molecules such as Notch, which is involved in cell fate decisions[33,34]. In both the P20 and the adult FACS-arrays, *Slc35d3* was consistently found to be the most striatonigral-enriched gene on the list (7.6-fold and 9.6-fold, respectively). Furthermore, our *in situ* hybridization at P20 showed that *Slc35d3* expression was highly restricted to the striatum with little expression elsewhere in the brain (**Fig. 5a**). Both RT-PCR and double *in situ* hybridization showed that *Slc35d3* expression was highly restricted to the striatonigral neurons (**Fig. 4**).

To provide *in vivo* genetic confirmation of the microarray result and to visualize the cell bodies and the axonal projection of the *Slc35d3*-expressing neurons in the brain, we developed BAC transgenic mice expressing EGFP under the promoter and regulatory elements of the *Slc35d3* gene (**Fig. 5b**). In these mice at P20, EGFP$^+$ neurons were highly restricted to the striatum (**Fig. 5c**). Furthermore, these EGFP$^+$ neurons had axons that terminated in the substantia nigra but not in the globus pallidus externa (GPe), and their cell bodies did not colocalize with the Penk1$^+$ striatopallidal neurons, demonstrating that EGFP is restricted to the striatonigral neurons (**Fig. 5d–f**). Together, these data showed that Slc35d3 is an uncharacterized nucleotide sugar transporter that is highly specific to the striatonigral neurons. Because homologs of Slc35d3 are rate-limiting regulators of protein glycosylation[32–35], these results indicate that cell type–specific protein glycosylation may have a key role in the function of the striatonigral neurons.

Ebf1 functions in striatonigral neuron differentiation

A transcription factor gene identified in the microarray analysis, *Zfp521* (also known as *Evi3*; refs. 36–38), was also particularly interesting because the transcriptional machinery controlling the differentiation and adult phenotypes of the MSN subtypes were unknown. This gene functionally interacts with Ebf1, a transcription factor controlling lineage specification and differentiation of B cells[39]. Moreover, Ebfaz, a protein highly related to Zfp521 (62% identify and 72% homology over the entire length of the proteins; refs. 36–38), physically interacts with Ebf1 and modulates its transcriptional activity[40,41]. The expression of both *Ebf1* and *Zfp521* is relatively specific to the striatum during development[42] (**Supplementary Fig. 3**). Therefore, we hypothesized that Zfp521 and Ebf1 may orchestrate a critical transcriptional program controlling the differentiation and function of the striatonigral neuron lineage. To test this hypothesis, we first confirmed, using both semiquantitative RT-PCR (**Fig. 6a**) and qRT-PCR (**Supplementary Table 2**), that the expression of both *Ebf1* and *Zfp521* was restricted to the striatonigral neurons at P20. qRT-PCR clearly demonstrated that

both genes were greatly enriched (>27-fold in two independent studies) in the striatonigral neurons, and the magnitude of the enrichment was comparable to that of three known cell type–specific genes tested: *Tac1* (substance P) in striatonigral neurons and *Drd2* and *Penk1* in striatopallidal neurons (**Supplementary Table 2**). The expression specificity of *Ebf1* in striatonigral neurons at P20 was further confirmed using double *in situ* hybridization (**Fig. 6b**).

Ebf1 knockout mice (*Ebf1*$^{-/-}$) have gross deficits in striatal MSN differentiation and survival[42] but it is unclear whether Ebf1 has any MSN subtype–specific function. We tested the hypothesis that Ebf1 has

Table 1 Genes differentially enriched in striatonigral and striatopallidal neurons

Gene	GeneBank	*P* value	Fold change P20	Fold change Adult	Validation	Striatum enriched
		Striatonigral neuron enriched				
Slc35d3	NM_029529	0.0000	7.6	9.6	RT/DI/Tg	+
Lrrn6c	NM_175516	0.0009	7.5	5.5		
Zfp521/Evi3	NM_145492	0.0001	4.9	8.1	RT	+
Stmn2	NM_025285	0.0000	3.3	3.3	RT/DI	
Gnb4	NM_013531	0.0000	3.3	3.0	RT/DI	+
Nrxn1	AK045351	0.0000	2.9	2.1		
	NM_020252	0.0005	2.4	4.1	RT	
Qk	NM_021881	0.0003	2.3	1.0	RT	
Kctd15	NM_146188	0.0011	2.3	1.0	RT	
Arx	NM_007492	0.0003	2.0	1.0		
		Striatopallidal neuron enriched				
Penk1	NM_001002927	0.0000	46.2	57.5	K	+
Adk	NM_134079	0.0000	3.6	2.6	RT	
Plxdc1	NM_028199	0.0001	3.6	3.1	RT	
Upb1	NM_133995	0.0006	3.6	3.3		
Adora2a	U05672	0.0001	3.2	2.8	K	+
Arpp19	NM_006628	0.0000	2.9	1.2	RT	+
EST	BC013561	0.0000	2.8	2.2		
RIKEN4933435E02	AK017066	0.0007	2.8	3.0		
Mest	NM_008590	0.0000	2.6	2.3		
Hspa1a	NM_010479	0.0002	2.5	1.6		
Map3k4	NM_011948	0.0005	2.4	2.1		
BC004044	NM_030565	0.0000	2.2	1.5		
Olfr1360	NM_146543	0.0005	2.2	5.0		
Rgs2	NM_009061	0.0043	2.2	1.7		
	NM_009061	0.0006	2.0	2.3	RT	+
RIKEN A930010C08	AK053689	0.0002	2.2	1.3		
Gnb5	BC016135	0.0000	2.1	1.2		+
Hist1h2bc	NM_023422	0.0000	2.1	1.0		
	NM_023422	0.0003	2.1	1.8		
RIKEN 1810027O10	XM_109683	0.0008	2.1	1.9		
Ctsz	NM_022325	0.0004	2.0	0.9	RT	
Dock3	NM_153413	0.0002	2.0	2.4	RT/DI	+
Utrn	AK012837	0.0003	2.0	1.1		
Calb1	NM_009788	0.0006	1.9	1.5		
RIKEN 1110032E23	AK008987	0.0000	1.9	1.3		
Ryr2	D38217	0.0002	2.2	1.1		
Slc6a15	BC076593	0.0002	2.0	1.4	RT	
Syt6	AK044551	0.0001	2.0	1.2		
EST	AC099603	0.0006	2.0	1.4		
Hbegf	NM_010415	0.0000	2.0	0.9	RT	
Zfp618	XM_143826	0.0004	1.9	1.5		
Zswim6	AK030163	0.0002	1.9	1.9	RT	+
Neto2	AK083010	0.0000	1.8	1.7		+
Nr4a1	NM_010444	0.0001	1.8	1.5		

Results are expressed as an average fold change in five (P20) and two (adult) independent experiments. Significance was calculated using paired *t*-test with a 5% false discovery rate. For the P20 FACS-arrays, genes with twofold or greater changes in four of five comparisons are shaded in blue; those with twofold or greater changes in three of five comparisons are shaded in orange. For the adult FACS-array, genes with twofold or greater changes in two of two comparisons are shaded in yellow. Microarray data validation was performed in independent samples using several different methods: semiquantitative and/or quantitative RT-PCR (RT); double *in situ* hybridizations (DI); and BAC-transgenesis (Tg). Two genes on the list are already known to be differentially expressed in the MSN subtypes (K). Genes with enriched expression in the striatum (see **Supplementary Fig. 2**) are indicated with a plus sign (+).

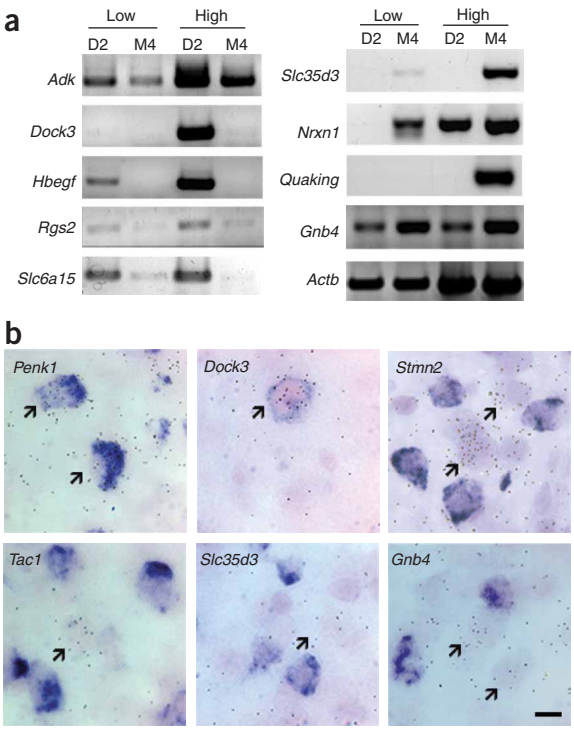

Figure 4 Independent validation of MSN subtype–specific genes. (**a**) Representative images of semiquantitative RT-PCR confirmation of differentially enriched genes in striatopallidal MSNs (left) and striatonigral (right) MSNs. *Actb* was used as a loading control (left). PCR products were amplified using two different cycles (low and high; **Supplementary Methods**). (**b**) Double *in situ* hybridizations (ISH) to illustrate cellular distribution of genes in the striatal MSN subtypes. Nonradioactive *in situ* hybridization with a *Penk1* probe (purple) was used to label the striatopallidal MSNs. Control radioactive ^{35}S *in situ* hybridization (black dots) with *Penk1* showed proper colocalization of radioactive grain clusters and nonradioactive staining in the striatopallidal MSNs, and with *Tac1* showed radioactive grain clusters outside the *Penk1*$^+$ striatopallidal MSNs. This method verified that *Dock3* colocalizes with *Penk1*$^+$ MSNs, whereas and *Slc35d3*, *Gnb4* and *Stmn2* do not. Arrows, radioactive grain clusters. Scale bar, 10 μm.

a critical role in striatonigral neuron differentiation by examining the development of MSN subtypes in the *Ebf1*$^{-/-}$ mice that were crossed with the *M4-EGFP* reporter mice, in which the striatonigral neurons and their axonal projections are labeled by EGFP (**Fig. 6c–e**; $n = 5$ for both *Ebf1*$^{-/-}$;*M4-EGFP* mice and the control *Ebf1*$^{+/+}$;*M4-EGFP* mice). At P14, an age when MSN subtype specification and axonal projection are mostly completed[28], we observed marked reduction in the number of EGFP$^+$ striatonigral MSNs in the *Ebf1*$^{-/-}$ striatum compared to wild-type controls (**Fig. 6d**) and, accordingly, in their axons and terminals in the substantia nigra (**Fig. 6e**). Notably, although striatonigral neurons in the entire striatum were affected in the *Ebf1*$^{-/-}$ mice, the dorsal striatum seemed to be more affected than the ventral striatum (both the nuclear accumbens and the olfactory tubercle) in these mice (**Supplementary Fig. 4** online). To ensure that the observed phenotype was not due to alterations in the expression of the *M4-EGFP* transgene, we stained the *Ebf1*$^{-/-}$ mice with antibodies to Tac1 (substance P), which is restricted to the striatonigral neuron axons and their terminals. We found a substantial reduction of Tac1$^+$ axonal terminal staining in the substantia nigra of *Ebf1*$^{-/-}$ mice compared to the wild-type controls (**Fig. 6e**). Contrary to the robust phenotype observed in the striatonigral neurons, the striatopallidal neurons were preferentially preserved in the *Ebf1*$^{-/-}$ mice at this age as indicated by greatly enriched Penk1$^+$ striatopallidal MSNs compared to the EGFP$^+$ striatonigral MSNs (**Fig. 6d**). To better visualize the striatopallidal neurons in the *Ebf1*$^{-/-}$ mice and to provide independent verification, we crossed these mice to the *D2-EGFP* reporter mice and found well-preserved EGFP$^+$ striatopallidal neurons throughout the striatum (**Fig. 6f**; $n = 3$ for both *Ebf1*$^{-/-}$;*D2-EGFP* mice and *Ebf1*$^{+/+}$;*D2-EGFP* control mice) and proper targeting and terminal arborization of their axons in the GPe in *Ebf1*$^{-/-}$ mice (**Fig. 6g**). Together, these results demonstrated that Ebf1 has an essential role in the differentiation of the striatonigral neuronal lineage but not in that of the striatopallidal neuronal lineage.

To investigate whether the selective striatonigral neuronal phenotype was due to the failure of MSN subtype specification or to the failure of neuronal differentiation, we examined *Ebf1*$^{-/-}$;*M4-EGFP* double-transgenic mice and *Ebf1*$^{+/+}$;*M4-EGFP* control mice at P0 ($n = 2$ for each genotype). We found that the striatonigral neurons and their axons were present in much greater numbers at this age than at P14

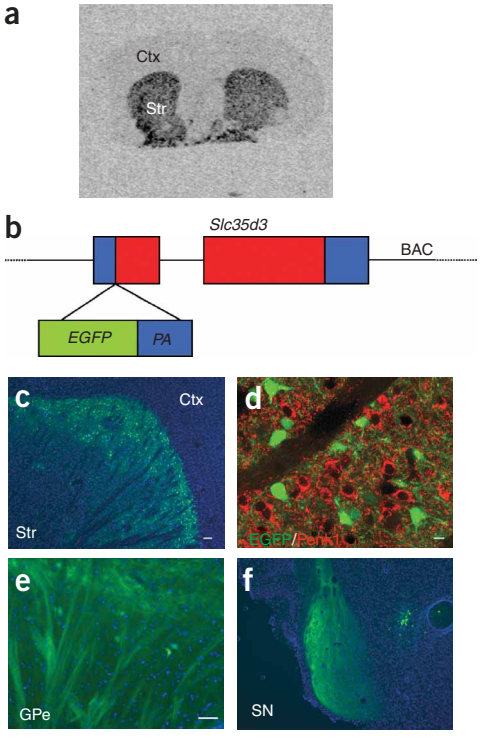

Figure 5 BAC transgenic validation of *Slc35d3* expression in the striatonigral neurons. (**a**) Radioactive *in situ* hybridization showed that *Slc35d3* expression at P20 was highly specific to the striatum (Str) with little expression in the cortex (Ctx) or elsewhere in the brain (data not shown). (**b**) Schematic drawing of the *Slc35d3-BAC-EGFP* transgene design. An *EGFP-polyA* (PA) sequence was inserted into 5′ untranslated region in exon 1 of the *Slc35d3* gene on the BAC. Blue boxes, untranslated regions. Red boxes, translated regions of *Slc35d3* gene. (**c–f**) EGFP expression in the basal ganglia of the P30 *Slc35d3-BAC-EGFP* mice (**c**) Striatum at low magnification. (**d**) Double immunofluorescence to demonstrate that striatal EGFP expression (green) in these mice does not colocalize with when stained with an antibody to Penk1 (anti-Penk1), which labels the striatopallidal neurons (red). (**e**,**f**) Axonal projections of the EGFP$^+$ MSNs in GPe (**e**) and substantia nigra (**f**) also verified that EGFP was expressed in the striatonigral neurons but not in the striatopallidal neurons in *Slc35d3-BAC-EGFP* mice. Scale bars: 100 μm in **c** and **f**; 50 μm in **e**; 10 μm in **d**.

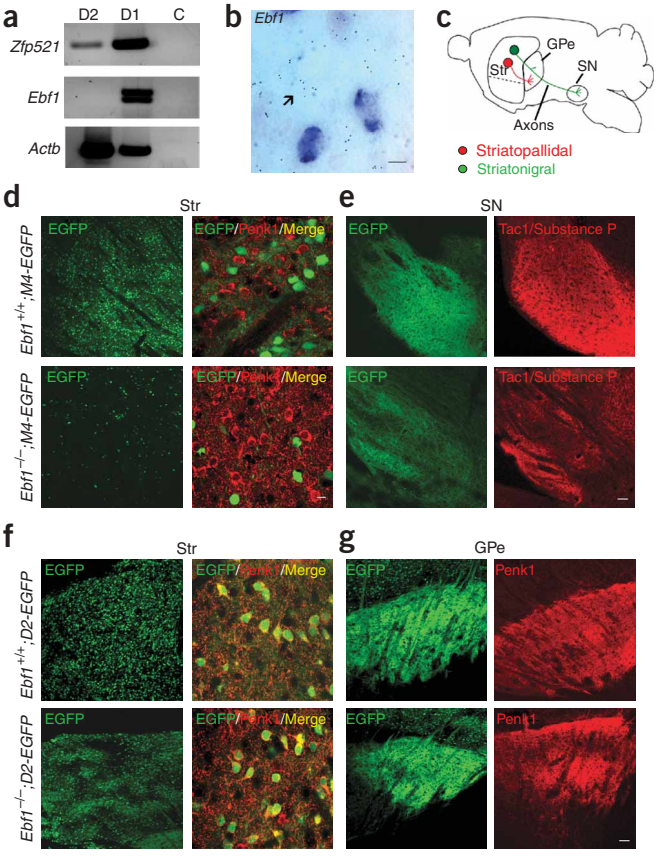

Figure 6 Ebf1 is involved in lineage-specific differentiation of striatonigral neurons. (**a**) Semiquantitative RT-PCR amplification of *Zfp521*, *Ebf1* and *Actb* (encoding β-actin) using *D2*- and *D1*- sorted RNA samples. (**b**) Double *in situ* hybridization using a ^{35}S-labeled radioactive *Ebf1* probe and a nonradioactive *Penk1* probe. Scale bar, 10 μm. (**c**) Schematic drawing of a sagittal mouse brain section illustrating projection of striatopallidal MSNs (red) to the GPe and of striatonigral MSNs (green) to the substantia nigra (and the internal segment of the globus pallidus). (**d**) *Ebf1*$^{-/-}$ mice had selective deficits in striatonigral neuron differentiation at P12–14. Sagittal sections of *Ebf1*$^{-/-}$;*M4-EGFP* mice and *Ebf1*$^{+/+}$;*M4-EGFP* control mice were examined. Low magnifications (left) revealed dramatic reduction of EGFP expression in *Ebf1*$^{-/-}$ striata. High magnification (right) showed that the *Ebf1*$^{-/-}$;*M4-EGFP* mice had fewer EGFP^{+} striatonigral neurons and more enriched Penk1^{+} striatopallidal neurons (red) compared to the control. (**e**) EGFP fluorescence (green) and Tac1 (substance P) immunofluorescent staining (red), independently demonstrated that the striatonigral neuron terminals in the substantia nigra were greatly reduced in *Ebf1*$^{-/-}$;*M4-EGFP* mice. (**f**) Both *Ebf1*$^{-/-}$;*D2-EGFP* mice and the *Ebf1*$^{+/+}$;*D2-EGFP* control mice at P12–14 had numerous EGFP^{+} striatopallidal MSNs at low magnification (left). These EGFP^{+} MSNs colocalized with Penk1 (red) at high magnification (right). (**g**) The striatopallidal axonal terminals in GPe, as indicated by direct EGFP fluorescence and by anti-Penk1 immunofluorescent staining (red), were intact in the *Ebf1*$^{-/-}$ mice compared to the control mice. Scale bars, 50 μm in all images in **d**–**g**, except for EGFP-Penk1 double-fluorescent images (10 μm).

(**Fig. 7a–f**). However, the EGFP^{+} striatonigral neurons had more loosely bundled axons compared to the wild type (**Fig. 7c,d**), and these axons did not form proper axonal terminal arborizations in the substantia nigra (**Fig. 7e,f**). These results showed that the striatonigral neurons are properly specified in the *Ebf1*$^{-/-}$ mice by P0 and their axons can reach the substantia nigra, but their axons and terminals in the substantia nigra do not develop properly. This striatonigral lineage–specific function of *Ebf1* is consistent with that of the *Ebf1* homolog *Unc-3*, which has been shown to regulate axonal development and neuronal subtype specification in *C. elegans*[43,44]. Thus, these genetic analyses revealed that *Ebf1* is a critical genetic determinant controlling the differentiation of the striatonigral projection neuron lineage.

DISCUSSION

The extraordinary complexity and heterogeneity of the mature mammalian brain create a major challenge for attempts to rapidly and reliably profile gene expression in a given neuronal population[1–3]. In this study, we demonstrated a simple yet powerful technology by which to purify genetically labeled neuronal populations in both juvenile and adult brains for gene expression profiling. Our work reveals several important features of this FACS-array technology and suggests its general utility. First, we demonstrate that FACS-purified mature juvenile and adult neurons clearly retain valuable cell type–specific transcripts that can be readily profiled and validated. Before our study, FACS purification and profiling of mature neuronal populations were thought to be difficult to achieve because these neurons are fragile and the process of dissociation and purification may result in the loss of cell type–specific transcripts and/or induce reactive changes including cell death. This work demonstrates that with the proper controls such as sorting for live EGFP^{+} and PI^{-} neurons, RNA quality control (for example, Agilent Bioanalyzer Picochip) and RT-PCR benchmarking for enrichment of known marker genes, FACS-purified mature neurons can be used to produce high quality, cell type–specific RNA samples suitable for microarray studies. *Post-hoc* analyses clearly showed that reactive gene expression changes such as cell death genes are not enriched with this method (**Supplementary Fig. 1**). Extensive follow-up studies

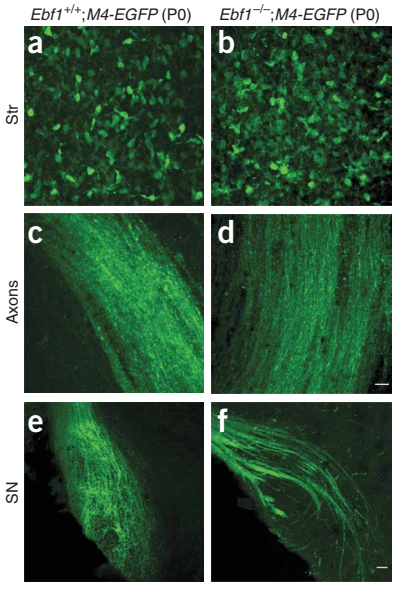

Figure 7 Striatonigral neuron axonal differentiation deficits in P0 *Ebf1*$^{-/-}$ mice. (**a**,**b**) In *Ebf1*$^{-/-}$;*M4-EGFP* mice, EGFP^{+} striatonigral neurons were much more abundant at P0 than at P12–14 (**Fig. 6**). (**c**–**f**) However, compared to the control mice, the EGFP^{+} striatonigral axons were less tightly bundled, and the axonal terminals did not form dense arborizations in the substantia nigra. These results demonstrated that striatonigral neurons were specified at P0 but did not properly differentiate in the *Ebf1*$^{-/-}$ mice. Scale bar: 20 μm in **a** and **b**; 50 μm in **c**–**f**.

showed that the majority of genes identified through FACS-array can be validated using independent methods. Moreover, the robustness and reproducibility of the FACS-array technology, even with smaller RNA samples representing 30–300 cells (see **Supplementary Methods** and **Supplementary Fig. 5** online), suggests that the FACS-array approach is applicable even for rare neuronal populations. Further, a significant advantage of the FACS-array technology is its usage of the already rich and rapidly expanding library of GENSAT BAC transgenic mice in which hundreds of different types of neurons are genetically labeled[12]. Thus, this technology is suitable for off-the-shelf, large-scale profiling of cell type–specific gene expression in many different types of neurons in the mammalian brain. Applications of the technology will permit immediate investigations of the dynamic changes of gene expression in a single neuronal population throughout the course of brain development, in behavioral protocols and during disease pathogenesis.

In addition to its technical advances, our study also provides important insights into the molecular composition of the two clinically important striatal projection neuron subtypes that comprise the direct and indirect pathways. Previous studies spanning more than a decade identified only six genes that are differentially expressed in these neuronal populations, all of which belong to two functional classes: neuropeptides and G-protein–coupled receptors[24–27]. Our comprehensive profiling identified nearly 40 differentially expressed genes and verified a large cross-section of these, including 16 new differentially enriched genes. These genes belong to new functional classes, including transcription factors, transporters, signal transduction molecules, RNA binding proteins and metabolic enzymes. GO analyses revealed that signal transduction (particularly G-protein–mediated pathways) was significantly different between these two functionally distinct striatal projection neurons. Because dopamine signaling is known to be mediated by G-protein–mediated pathways[13,14,31], it will be interesting to further investigate the possible involvement of these differentially expressed signaling molecules to determine if they contribute to differential dopamine signaling in the striatal projection neuron subtypes. Furthermore, our genetic analyses using BAC transgenesis demonstrate that *Slc35d3* encodes a nucleotide sugar transporter and is specifically expressed in the striatonigral neurons. Because this family of transporters includes rate-limiting regulators of protein glycosylation[32–35], this suggests that Slc35d3-mediated protein glycosylation may be critical to the proper function of the striatonigral neurons.

Before this study, lineage-specific transcription factors controlling the specification, differentiation and maintenance of the striatal projection neuron subtypes were completely unknown. Here we established Ebf1 as a lineage-specific transcription factor essential to the differentiation of striatonigral neurons. This result is consistent with the known role of *Ebf1* and its homologs in the specification and differentiation of B cells[39] and sensory neuronal subtypes in *C. elegans*[43,44]. Because both *Ebf1* and its regulator *Zfp521* are highly restricted to the B cell lineage[36–39] and to the striatonigral neuronal lineage, this study also revealed an unexpected parallel between the molecular programs regulating lineage-specific development in lymphocytes and striatal projection neurons. Further identification of upstream regulators and downstream transcriptional targets of Ebf1 in striatonigral neurons and further molecular and genetic analyses of *Zfp521* may elucidate the central molecular program regulating the differentiation and function of the striatonigral neurons.

Finally, our results have important implications for the study of neurological and psychiatric disorders targeting the basal ganglia by providing a potentially important set of candidate genes to consider when studying the genetic basis of these disorders. It is notable that two of the identified genes have some known association with movement disorders. First, one study found that translocation and fusion of *DOCK3* with an uncharacterized solute transporter (*SLC9A9*) co-segregates with an attention deficit and hyperactivity disorder (ADHD)-like clinical syndrome in a family[45], but this study could not distinguish which one of the two genes was responsible. Because we have found *Dock3* to be selectively expressed in striatopallidal neurons that normally inhibit movement, our study suggests that the disruption of human *DOCK3* is probably the primary cause of the observed ADHD-like phenotype in the affected family. Second, Sydenham chorea, a childhood hyperkinetic movement disorder with predisposition to OCD and ADHD, is linked to antibodies to basal ganglia that recognize sugar moieties of glycoproteins on MSNs (refs. 46–48). Our study also demonstrates for the first time a new nucleotide sugar transporter, whose expression is highly restricted to the striatonigral neurons. This suggests that further investigation of Slc35d3-mediated, striatonigral-specific protein glycosylation may provide molecular insights into the pathogenesis of Sydenham chorea. Finally, our study provides a new set of molecular targets to screen for therapeutic compounds that can selectively modulate the output of either the direct or indirect pathways in the basal ganglia, which could help to ameliorate the functional imbalance of these pathways in a variety of movement and psychiatric disorders.

METHODS

Animals. *Drd2-EGFP*, *Drd1a-EGFP* and *Chrm4-EGFP* mice on the FVB/N inbred background were obtained from N. Heintz and the NINDS/GENSAT program at Rockefeller University[12] . P20 and 2-month-old mice were used for the study. *Ebf1* knockout mice[39] on a mixed 129/C57Blk/6 background were obtained from R. Grosschedl (Max-Planck-Institute of Immunobiology, Freiburg, Germany). Mice were maintained in a 12-h light-dark cycle and housed 1–4 per cage with food and water *ad libitum*. All animal protocols were in accordance with the US National Institutes of Health Guide for the Care and Use of Laboratory Animals and were approved by the Institutional Animal Care and Use Committee at UCLA.

Enzymatic dissociation and FACS purification of striatal neurons. Brains from three or four transgenic mice around P20 or 2 months of age were dissected and sectioned in the coronal plane at 500 μm on a vibratome. The striata were then dissected and dissociated using the Papain Dissociation System (Worthington Biochem; **Supplementary Methods**). Cells were resuspended in buffer media (L15-CO_2 without phenol, 1× penicillin and streptomycin, 10 mM Hepes, 25 μg ml^{-1} DNase and 1 mg ml^{-1} bovine serum albumin) and filtered through a 70-μm mesh. Cells were treated with PI (20 μg ml^{-1}) to label dead cells and sorted on a FACSVantage SE cell sorter (Becton Dickson) for fluorescein-5-isothiocyanate (FITC) signals (EGFP) and phycoerythrin (PE) signals (PI). Wild-type striatal cells were used to calibrate the FITC and PE signals. Cells with high FITC signals (FITC $>10^{3.5}$) and negative PI signals were selected. Routinely, 5,000–10,000 striatal MSNs were obtained in each sort from the *D1*-, *D2*- and *M4* mice. For cell viability and imaging of pre- and postsorted neurons, see **Supplementary Methods**.

RNA preparation and cRNA amplification. RNA extraction was performed with PicoPure RNA isolation kit (Arcturus) with a DNase I digestion (Qiagen). RNA quality and relative concentration were confirmed on the Picochip (Agilent). We used 3 ng of RNA as the initial starting template, which underwent two rounds of *in vitro* transcription and was labeled with Cy-3 or Cy-5 cytidine -5'-triphosphate (CTP) using the low input fluorescent linear amplification kit (Agilent). For detailed cRNA amplification, see **Supplementary Methods**. Labeled cRNA was cleaned with RNeasy MiniElute kit (Qiagen) and eluted in a 30 μl volume. The final labeled cRNA concentration was verified (Nanodrop) and RNA quality was checked on a Bioanalyzer Nanochip (Agilent).

Agilent microarrays. All experiments were performed on mouse I and mouse developmental microarrays (Agilent). Microarray hybridization and scanning

was performed according to standard protocols (Agilent). Both platforms contained a total of 41,147 distinct probes. In our analysis, we did not include 3,458 (15.1%) intron-specific and 494 (2.4%) error probes (including cross-reactive, DNA segments, non–mouse genes, wrong strand and repeat sequences). Due to partial overlap in mouse I and developmental slides, the total list of genes corresponded to 19,755 (48.0%) unique genes with known full-length cDNA sequence (including RIKEN genes) and an additional 8,927 (21.7%) expressed sequence tags (ESTs).

Microarray data analysis. Data analysis of homotypic comparisons (biological replicates) was performed in the TIGR TM4 microarray statistical package[49]. For identification of differential expression in heterotypic comparisons (different neuronal subtypes), genes were selected based on two criteria: the fold change (>2.0-fold) and the significance of their expression changes ($P<0.01$). Because theoretically no genes should be differentially expressed in homotypic comparisons, this allows one to measure the false positive level and derive a threshold that corresponds to a given level of confidence[29]. P-values were computed using the maximum number of permutations of the data for each gene in TM4[49]. For the most stringent analysis all genes with expression changes above 2 fold in at least four out of five experiments were selected. We also used more relaxed criteria in which only three out of five experiments acceded 2.0 fold expression change (this always included at least one D1/D2 experimental replicate) (**Table 1**). For further details on data analyses, see **Supplementary Methods**. The original microarray data in this study are being deposited at the OMNIBUS at NCBI and at our lab website (http://yanglab.npih.ucla.edu).

Semiquantitative and quantitative RT-PCR. Isolated RNA underwent one round of *in vitro* transcription using the Low Input Linear Fluorescence kit (Agilent technologies) followed by reverse transcription (Qiagen). cDNA quantity was normalized for each sample using an *Actb* dilution series. Semiquantitative PCR reactions were carried out at 2 different cycles for each gene. qRT-PCRs were performed using Taqman 7700 Thermal Cycler and Taqman Gene Expression Assays (Applied Biosystems). For more details on the RT-PCR methods and primers used, see **Supplementary Methods** and **Supplementary Table 3** online.

Double *in situ* hybridization. Antisense-RNA probes for each gene of interest (labeled with ^{35}S uridine-5'-triphosphate (UTP), Perkin-Elmer) and the *Penk1* probe (labeled with Digoxigenin-UTP, Roche) were prepared. Fresh-frozen brain sections from P20 mice were used for *in situ* hybridization. For detailed *in situ* hybridization methods, see **Supplementary Methods**.

Immunofluorescence. Sagittal sections were incubated in 1:1,000–1:2,000 of rabbit antibody to met-enkephalin[50], 1:400 of rat antibody to substance P (Chemicon) or 1:400 rabbit antibody to GFP (Molecular Probes) overnight at room temperature (22 °C). Immunoreactivity was visualized using biotinylated and fluorescent secondary antibodies (Chemicon and Molecular Probes) and images were analyzed on a Zeiss LSM 510 Meta confocal microscope or a Zeiss Axioscope II microscope. For a detailed immunofluorescence protocol, see **Supplementary Methods**.

Generation of Slc35d3 BAC transgenic mice. An *EGFP* marker gene was inserted in front of the endogenous ATG in exon 1 of *Slc35d3* in a 196 kilobase (kb) mouse BAC (RP23-344M6) using the RecA-based BAC modification protocol[9–11]. The PCR primers used to amplify the homology arm A are as follows: Slc35d3-A5′ Flank: 5′-AGGCGCGCCAGCTGTGCAGGGGATCCCC CAGCA-3′; Slc35d- A5′: 5′-AGGCGCGCCGCACCCCGCTGCTCTGCCACT GTG-3′; Slc35d3-3′: 5′-TCCCCCCGGGACCCCGCCGTGCGGAGCTCG-3′. DNA from the modified BAC was purified and microinjected into fertilized eggs from the inbred FvB mouse strain. One transgenic founder was identified by PCR analyses, and the offsprings in this BAC transgenic mouse line were used for detailed analyses.

Note: Supplementary information is available on the Nature Neuroscience website.

ACKNOWLEDGMENTS

We would like to thank N. Heintz (Rockefeller University) and the National Institute of Neurological Disorders and Stroke (NINDS) Gene Expression Nervous System Atlas (GENSAT) program for providing the BAC transgenic mice; R. Grosschedl (Max-Planck-Institute of Immunobiology, Freiburg, Germany) for the *Ebf1* knockout mice; M.S. Levine for equipment use; C. Evans for the met-Enkephalin antibody; D. Anderson (California Institute of Technology) for advice on cell dissociation; and S.L. Zipursky, A. Silva, D.E. Krantz, Y.E. Sun, M.S. Levine and members of the Yang lab for discussions. We would like to thank the UCLA Jonsson Comprehensive Cancer Center and Center for AIDS Research Flow Cytometry Core Facility, and UCLA NINDS/National Institute of Mental Health (NIMH) DNA Microarray Core Facility for their services. X.W.Y. is supported by Semel Institute for Neuroscience and Human Behaviors, NINDS (NS049501 and NS047391) and the Hereditary Disease Foundation, and by pilot grants from UCLA Hatos Center for Neuropharmacology (National Institute of Drug Abuse P50DA05010) and UCLA Brain Research Institute (supported by the Employees Charity Organization of Northrup Grumman). M.K.L. and M.G. are supported by UCLA Mental Retardation Research Center training grants (5T32HD007032 from National Institute of Child Health and Human Development). M.G. is also supported by UCLA Center for Neurobehavioral Genetics (5T32NS048004 from NINDS). D.H.G. is supported by NINDS/NIMH U24 NS43562. S.L.K. is supported by the French Foundation for Alzheimer's Research.

COMPETING INTERESTS STATEMENT

The authors declare that they have no competing financial interests.

Published online at http://www.nature.com/natureneuroscience/
Reprints and permissions information is available online at http://npg.nature.com/reprintsandpermissions/

1. Dougherty, J.D. & Geschwind, D.H. Progress in realizing the promise of microarrays in systems neurobiology. *Neuron* **45**, 183–185 (2005).
2. Mirnics, K. & Pevsner, J. Progress in the use of microarray technology to study the neurobiology of disease. *Nat. Neurosci.* **7**, 434–439 (2004).
3. Cao, Y. & Dulac, C. Profiling brain transcription: neurons learn a lesson from yeast. *Curr. Opin. Neurobiol.* **11**, 615–620 (2001).
4. Tietjen, I. *et al.* Single-cell transcriptional analysis of neuronal progenitors. *Neuron* **38**, 161–175 (2003).
5. Kamme, F. *et al.* Single-cell microarray analysis in hippocampus CA1: demonstration and validation of cellular heterogeneity. *J Neurosci.* **23**, 3607–3615 (2003).
6. Arlotta, P. *et al.* Neuronal subtype-specific genes that control corticospinal motor neuron development in vivo. *Neuron* **45**, 207–221 (2005).
7. Loconto, J. *et al.* Functional expression of murine V2R pheromone receptors involves selective association with the M10 and M1 families of MHC class Ib molecules. *Cell* **112**, 607–618 (2003).
8. Molyneaux, B.J., Arlotta, P., Hirata, T., Hibi, M. & Macklis, J.D. Fezl is required for the birth and specification of corticospinal motor neurons. *Neuron* **47**, 817–831 (2005).
9. Heintz, N. BAC to the future: the use of bac transgenic mice for neuroscience research. *Nat. Rev. Neurosci.* **2**, 861–870 (2001).
10. Yang, X.W., Model, P. & Heintz, N. Homologous recombination based modification in *Escherichia coli* and germline transmission in transgenic mice of a bacterial artificial chromosome. *Nat. Biotechnol.* **15**, 859–865 (1997).
11. Gong, S., Yang, X.W., Li, C. & Heintz, N. Highly efficient modification of bacterial artificial chromosomes (BACs) using novel shuttle vectors containing the R6Kgamma origin of replication. *Genome Res.* **12**, 1992–1998 (2002).
12. Gong, S. *et al.* A gene expression atlas of the central nervous system based on bacterial artificial chromosomes. *Nature* **425**, 917–925 (2003).
13. Gerfen, C.R. The neostriatal mosaic: multiple levels of compartmental organization. *Trends Neurosci.* **15**, 133–139 (1992).
14. Graybiel, A.M. The basal ganglia. *Curr. Biol.* **10**, R509–R511 (2000).
15. Packard, M.G. & Knowlton, B.J. Learning and memory functions of the basal ganglia. *Annu. Rev. Neurosci.* **25**, 563–593 (2002).
16. Albin, R.L., Young, A.B. & Penney, J.B. The functional anatomy of basal ganglia disorders. *Trends Neurosci.* **12**, 366–375 (1989).
17. DeLong, M.R. Primate models of movement disorders of basal ganglia origin. *Trends Neurosci.* **13**, 281–285 (1990).
18. Wichmann, T. & DeLong, M.R. Pathophysiology of Parkinson's disease: the MPTP primate model of the human disorder. *Ann. NY Acad. Sci.* **991**, 199–213 (2003).
19. Chao, J. & Nestler, E.J. Molecular neurobiology of drug addiction. *Annu. Rev. Med.* **55**, 113–132 (2004).
20. Graybiel, A.M. & Rauch, S.L. Toward a neurobiology of obsessive-compulsive disorder. *Neuron* **28**, 343–347 (2000).
21. Saka, E. & Graybiel, A.M. Pathophysiology of Tourette's syndrome: striatal pathways revisited. *Brain Dev.* **25** suppl. Suppl 1, S15–S19 (2003).
22. Meyer-Lindenberg, A. *et al.* Reduced prefrontal activity predicts exaggerated striatal dopaminergic function in schizophrenia. *Nat. Neurosci.* **5**, 267–271 (2002).
23. Rogers, M.A., Bradshaw, J.L., Pantelis, C. & Phillips, J.G. Frontostriatal deficits in unipolar major depression. *Brain Res. Bull.* **47**, 297–310 (1998).
24. Gerfen, C.R. *et al.* D1 and D2 dopamine receptor-regulated gene expression of striatonigral and striatopallidal neurons. *Science* **250**, 1429–1432 (1990).
25. Hersch, S.M. *et al.* Electron microscopic analysis of D1 and D2 dopamine receptor proteins in the dorsal striatum and their synaptic relationships with motor corticostriatal afferents. *J. Neurosci.* **15**, 5222–5237 (1995).

26. Schiffmann, S.N. & Vanderhaeghen, J.J. Adenosine A2 receptors regulate the gene expression of striatopallidal and striatonigral neurons. *J. Neurosci.* **13**, 1080–1087 (1993).
27. Ince, E., Ciliax, B.J. & Levey, A.I. Differential expression of D1 and D2 dopamine and m4 muscarinic acetylcholine receptor proteins in identified striatonigral neurons. *Synapse* **27**, 357–366 (1997).
28. Fishell, G. & van der Kooy, D. Pattern formation in the striatum: neurons with early projections to the substantia nigra survive the cell death period.. *J. Comp. Neurol.* **312**, 33–42 (1991).
29. Sabatti, C., Karsten, S.L. & Geschwind, D.H. Thresholding rules for recovering a sparse signal from microarray experiments. *Math. Biosci.* **176**, 17–34 (2002).
30. Dennis, G. Jr. *et al.* DAVID: database for annotation, visualization, and integrated discovery. *Genome Biol.* **4**, 3 (2003).
31. Svenningsson, P. *et al.* DARPP-32: an integrator of neurotransmission. *Annu. Rev. Pharmacol. Toxicol.* **44**, 269–296 (2004).
32. Ishida, N. & Kawakita, M. Molecular physiology and pathology of the nucleotide sugar transporter family (SLC35). *Pflugers Arch.* **447**, 768–775 (2004).
33. Goto, S. *et al.* UDP-sugar transporter implicated in glycosylation and processing of Notch. *Nat. Cell Biol.* **3**, 816–822 (2001).
34. Selva, E.M. *et al.* Dual role of the fringe connection gene in both heparan sulphate and fringe-dependent signalling events. *Nat. Cell Biol.* **3**, 809–815 (2001).
35. Berninsone, P. *et al.* SQV-7, a protein involved in *Caenorhabditis elegans* epithelial invagination and early embryogenesis, transports UDP-glucuronic acid, UDP-N- acetylgalactosamine, and UDP-galactose. *Proc. Natl. Acad. Sci. USA* **98**, 3738–3743 (2001).
36. Warming, S. *et al.* Evi3, a common retroviral integration site in murine B-cell lymphoma, encodes an EBFAZ-related Kruppel-like zinc finger protein. *Blood* **101**, 1934–1940 (2003).
37. Bond, H.M. *et al.* Early hematopoietic zinc finger protein (EHZF), the human homolog to mouse Evi3, is highly expressed in primitive human hematopoietic cells. *Blood* **103**, 2062–2070 (2004).
38. Hentges, K.E. *et al.* Evi3, a zinc-finger protein related to EBFAZ, regulates EBF activity in B-cell leukemia. *Oncogene* **24**, 1220–1230 (2005).
39. Lin, H. & Grosschedl, R. Failure of B-cell differentiation in mice lacking the transcription factor EBF. *Nature* **376**, 263–267 (1995).
40. Tsai, R.Y. & Reed, R.R. Cloning and functional characterization of Roaz, a zinc finger protein that interacts with O/E-1 to regulate gene expression: implications for olfactory neuronal development. *J. Neurosci.* **17**, 4159–4169 (1997).
41. Hata, A. *et al.* OAZ uses distinct DNA- and protein-binding zinc fingers in separate BMP-Smad and Olf signaling pathways. *Cell* **100**, 229–240 (2000).
42. Garel, S., Marin, F., Grosschedl, R. & Charnay, P. Ebf1 controls early cell differentiation in the embryonic striatum. *Development* **126**, 5285–5294 (1999).
43. Prasad, B.C. *et al.* unc-3, a gene required for axonal guidance in *Caenorhabditis elegans*, encodes a member of the O/E family of transcription factors. *Development* **125**, 1561–1568 (1998).
44. Kim, K., Colosimo, M.E., Yeung, H. & Sengupta, P. The UNC-3 Olf/EBF protein represses alternate neuronal programs to specify chemosensory neuron identity. *Dev. Biol.* **286**, 136–148 (2005).
45. de Silva, M.G. *et al.* Disruption of a novel member of a sodium/hydrogen exchanger family and DOCK3 is associated with an attention deficit hyperactivity disorder-like phenotype. *J. Med. Genet.* **40**, 733–740 (2003).
46. Martino, D. & Giovannoni, G. Antibasal ganglia antibodies and their relevance to movement disorders. *Curr. Opin. Neurol.* **17**, 425–432 (2004).
47. Church, A.J. *et al.* Anti-basal ganglia antibodies in acute and persistent Sydenham's chorea. *Neurology* **59**, 227–231 (2002).
48. Kirvan, C.A., Swedo, S.E., Heuser, J.S. & Cunningham, M.W. Mimicry and autoantibody-mediated neuronal cell signaling in Sydenham chorea. *Nat. Med.* **9**, 914–920 (2003).
49. Saeed, A.I. *et al.* TM4: a free, open-source system for microarray data management and analysis. *Biotechniques* **34**, 374–378 (2003).
50. Tecott, L.H., Rubenstein, J.L., Paxinos, G., Evans, C.J., Eberwine, J.H. & Valentino, K.L. Developmental expression of proenkephalin mRNA and peptides in rat striatum. *Brain Res. Dev. Brain Res.* **49**, 75–86 (1989).